**Astronomy
&
Astrophysics**

The spatial clustering of distant, $z \sim 1$, early-type galaxies

E. Daddi[1], T. Broadhurst[2], G. Zamorani[3], A. Cimatti[4], H. Röttgering[5], and A. Renzini[2]

[1] Università degli Studi di Firenze, Dipartimento di Astronomia e Scienza dello Spazio, Largo E. Fermi 5,
50125 Firenze, Italy
[2] European Southern Observatory, 85748 Garching, Germany
[3] Osservatorio Astronomico di Bologna, Via Ranzani 1, 40127 Bologna, Italy
[4] Osservatorio Astrofisico di Arcetri, Largo E. Fermi 5, 50125 Firenze, Italy
[5] Sterrewacht Leiden, Postbus 9513, 2300 RA Leiden, The Netherlands

Abstract. We examine the spatial clustering of extremely red objects (EROs) found in a relatively large survey of 700 arcmin^2, containing 400 galaxies with $R - Ks > 5$ to $Ks = 19.2$. A comoving correlation length $r_0 = 12 \pm 3\ h^{-1}$ Mpc is derived, under the assumption that the selection function is described by a passively evolving early-type galaxy population, with an effective redshift of $z \sim 1.2$. This correlation length is very similar to that of local L^* elliptical galaxies implying, at face value, no significant clustering evolution in comoving coordinates of early-type galaxies to the limiting depth of our sample, $z \sim 1.5$. A rapidly evolving clustering bias can be designed to reproduce a null result; however, our data do not show the corresponding strong reduction in the average population density expected for consistency with underlying growth of the mass-function. We discuss our data in the context of recent ideas regarding bias evolution.

The uncertainty we quote on r_0 accounts for the spikey redshift distribution expected along relatively narrow sightlines, which we quantify with detailed simulations. This is an improvement over the standard use of Limber's equation which, because of its implicit assumption of a smooth selection function, underestimates the true noise by a factor of ≈ 3 for the parameters of our survey. We propose a general recipe for the analysis of angular clustering, suggesting that any measurement of the angular clustering amplitude, A, has an intrinsic additional uncertainty of $\sigma_A/A = \sqrt{AC}$, where AC is the appropriate integral constraint.

Key words. cosmology: large-scale structure of Universe – galaxies: evolution – galaxies: elliptical and lenticular, cD – galaxies: formation – galaxies: fundamental parameters

1. Introduction

The evolution of the galaxy two-point correlation function provides important insights into the nature of galaxy formation and evolution (Peebles 1980; Efstathiou et al. 1991). The shape and normalization of this function depends on both the cosmic growth of mass structures and on the details of how galaxies trace mass at different epochs – the bias evolution. Measurements of the clustering evolution of galaxies of different luminosites and morphological types help constraining how, when and where they were formed.

In the last few years, a number of investigations of the spatial clustering of distant galaxies has been carried out. A marked decline in the amplitude of the spatial correlation function has been reported to $z \sim 1$, for magnitude selected samples of field galaxies (Le Fevre et al. 1996; Carlberg et al. 1997; Hogg et al. 2000), consistent with a stable clustering scenario. This decline seems to

reverse towards high–z, given the strong clustering reported for Lyman-Break Galaxies (LBG's hereafter) at $z = 3$ (Giavalisco et al. 1998; Adelberger et al. 1998).

Recently, Daddi et al. (2000b) (D2000 hereafter) detected a large angular clustering signal from extremely red, $R - Ks > 5$, galaxies (EROs) obtained from a K-selected survey over 700 arcmin^2. The angular clustering of EROs was found to be an order of magnitude larger than the full K-magnitude selected galaxies, and an increase of the clustering signal was detected with increasing Ks luminosity and increasing $R - Ks$ color (D2000). A similarly large angular clustering amplitude for EROs has been reported by McCarthy et al. (2000) in an imaging survey of red galaxies detected in an H–selected sample.

From the selection criteria it is known that EROs can be high-redshift passively evolving ellipticals or dusty starbursts, and examples of both classes exist (see e.g. D2000 for more details). It is becoming clear however, that the bulk of the ERO population is probably dominated by the former class: Broadhurst & Bouwens (2000), Moriondo et al. (2000) and Stiavelli & Treu (2000) have concluded

from independent datasets that most (∼70%) such objects have De Vaucouleurs profiles, with only about 15% of them displaying irregular or disturbed morphologies, expected for dusty starburst systems (the remaining 15% has a disk-like exponential profile). The existing spectroscopic results for single objects or for small samples of EROs support this conclusion (Spinrad et al. 1997; Soifer et al. 1999; Cimatti et al. 1999; Liu et al. 2000). Spectroscopy of flux-limited samples of K selected galaxies generally suffer from incompleteness of the optically reddest galaxies but the weight of evidence is that most of the reddest objects have spectra consistent with early-type galaxies, up to the effective spectroscopic limit of $z \sim 1.3$ for absorption-line work (Cohen et al. 1999; Eisenhardt et al. 1998; Cimatti 2001). These surveys also broadly show that the EROs of known redshift are in the range $0.8 \lesssim z \lesssim 1.5$, consistent with expectations for passively evolving ellipticals based on an extrapolation of the local luminosity function with passive evolution (Sect. 3).

Even if a few EROs have been identified as counterparts of SCUBA sources (Smail et al. 1999; Gear et al. 2000), SCUBA observations of complete ERO samples show no frequent detections (Mohan et al. 2001, in preparation) reinforcing the idea that dusty HR10-like objects (Cimatti et al. 1998; Dey et al. 1999; Andreani et al. 2000) are rare among EROs. It is therefore reasonable to conclude that with $K \lesssim 19$ EROs we are observing the clustering signal of predominantly distant early-type galaxies.

Here we take the angular correlation function measurements of the EROs and a plausible estimate of their selection function to derive their spatial clustering amplitude. The 3D correlation length of EROs should thus produce constraints on the evolution of the clustering of early-type galaxies, a population of objects which is likely to have formed in the highest amplitude perturbations and to be positively biased with respect to the general galaxy population and to the overall distribution of mass. The evolution of the correlation amplitude of early-type galaxies is an observable which is independent of measurements of the evolution of their comoving number density, providing therefore a complementary mean to examine the rate of evolution. Constraints on the density evolution of EROs have been sought previously in response to predictions of CDM models (Baugh et al. 1996; Kauffmann 1996). Early work based on small fields claimed observational evidence for a sharp decline in space density of early type galaxies, while more recent estimates based on deeper and more complete samples are consistent with a constant comoving density of this population up to at least $z \sim 1.3$, and imply a typical formation redshift of the stars in these galaxies not less than $z_{\rm f} \sim 2.5$ assuming passive evolution (see Daddi et al. 2000a for a complete discussion). Hence it is very important to obtain information regarding the clustering evolution to independently address this important question. Here we analyze together both these questions of clustering and density evolution of EROs, with the largest complete sample of relevant data.

In Sect. 2 we describe the standard Limber's equation formalism. Section 3 derives order-of-magnitude results on the correlation length r_0 that confirm the interpretation of EROs as high–z early type galaxies and justify our assumed redshift distribution. Section 4 present the r_0 estimates based on Limber's equation. In Sect. 5 we discuss the limitation of the standard approach and we use numerical simulations to find the definitive constraint on the correlation length, that differs significantly from the Limber's equation results. We discuss the general implications of our findings for the clustering analysis on small areas. We than compare in Sect. 6 our estimates of the correlation length of distant ellipticals to the measurements in the local universe and to theoretical models predictions. Our conclusions are presented in Sect. 7.

All the scales quoted in the paper are given in comoving units. Three cosmological models have been considered: a Λ-flat universe ($\Omega_{\rm m} = 0.3$, $\Omega_{\Lambda} = 0.7$, $h = 0.7$), an open universe ($\Omega_{\rm m} = 0.3$, $\Omega_{\Lambda} = 0$, $h = 0.7$) and an Ω-flat universe ($\Omega_{\rm m} = 1$, $\Omega_{\Lambda} = 0$, $h = 0.5$). $H_0 = 100h$ km s^{-1} Mpc^{-1}.

2. Limber's equation and the spatial correlation length

The angular two point correlation function $w(\theta)$ is related to its real space analogous $\xi(r)$ by Limber's equation (Peebles 1980). In the case of small angles ($\theta \ll 1$), if both w and ξ have power law shapes, writing $\xi(z) = (r/r_0(z))^{-\gamma}$ (with $r_0(z)$ being the comoving correlation length at redshift z, and r the comoving distance), the Limber's equation becomes:

$$w(\theta) = \sqrt{\pi} \frac{\Gamma((\gamma - 1)/2)}{\Gamma(\gamma/2)} \frac{\int g(z)(\mathrm{d}N/\mathrm{d}z)^2 r_0(z)^{\gamma} \mathrm{d}z}{[\int (\mathrm{d}N/\mathrm{d}z)\mathrm{d}z]^2} \theta^{1-\gamma} \quad (1)$$

where $\mathrm{d}N/\mathrm{d}z$ is the redshift selection function of the sample, which in the limit of a large number of objects coincides with the observed redshift distribution. The function $g(z)$ depends only on the cosmology:

$$g(z) = (\mathrm{d}x/\mathrm{d}z)^{-1} x^{1-\gamma} F(x) \quad (2)$$

where x and $F(x)$ are defined with the metric:

$$\mathrm{d}s^2 = c^2 \mathrm{d}t^2 - a^2 [\mathrm{d}x^2/F(x)^2 + x^2(\mathrm{d}\theta^2 + \sin^2 \theta \mathrm{d}\phi^2)].$$

If we define:

$$r_{0,\rm eff}^{\gamma} = \int g(z)(\mathrm{d}N/\mathrm{d}z)^2 r_0(z)^{\gamma} \mathrm{d}z \ / \ \int g(z)(\mathrm{d}N/\mathrm{d}z)^2 \quad (3)$$

then by using Eq. (1) and with $w(\theta) = A\theta^{1-\gamma}$ we have:

$$A = r_{0,\rm eff}^{\gamma} B \quad (4)$$

$$B = \sqrt{\pi} \frac{\Gamma((\gamma - 1)/2)}{\Gamma(\gamma/2)} \frac{\int g(z)(\mathrm{d}N/\mathrm{d}z)^2 \mathrm{d}z}{[\int (\mathrm{d}N/\mathrm{d}z)\mathrm{d}z]^2}. \quad (5)$$

Thus, knowledge of a measured or assumed redshift distribution allows us to relate the angular clustering amplitudes A to the 3D correlation length $r_{0,\rm eff}$. If $\mathrm{d}^2 r_0(z)^{\gamma}/\mathrm{d}z^2$

is negligible in the relevant redshift range, then $r_{0,\mathrm{eff}} = r_0(z_{\mathrm{eff}})$ with:

$$z_{\mathrm{eff}} = \int z W(z) \mathrm{d}z \tag{6}$$

$$W(z) = g(z)(\mathrm{d}N/\mathrm{d}z)^2 / \int g(z)(\mathrm{d}N/\mathrm{d}z)^2 \mathrm{d}z. \tag{7}$$

This *inversion* process provides a weighted estimate of r_0 over the probed redshift range. In the following, we will refer generically to r_0 as $r_{0,\mathrm{eff}} = r_0(z_{\mathrm{eff}})$, bearing in mind, anyway, the effect of Eqs. (3) and (6). For consistency with D2000, where the clustering amplitudes were fitted with $w(\theta) \propto \theta^{-0.8}$, we assume $\gamma = 1.8$ for our analysis, consistent with most previous observations (see e.g. Roche & Eales 1999). In the following we will quote the values for the amplitude of the angular two-point correlation function as measured (or extrapolated) to 1 degree, i.e. $A \equiv A(1^\circ)$.

3. The effects of the selection function

To derive 3D information from the angular correlation measurements a selection function for EROs must be supplied. As discussed in the introduction, strong evidence exist that the bulk of EROs is made of early type galaxies.

The strong angular clustering of EROs reported by D2000 and McCarthy et al. (2000), independently supports this same conclusion. In fact, early-type galaxies in the local universe are known to prefer high density environments (Dressler 1980) and to have much larger correlation lengths than late-type galaxies ($r_0 \gtrsim 7$–8 versus $r_0 \lesssim 5$; Davis & Geller 1976; Giovanelli et al. 1986; Loveday et al. 1995) and than dusty starburst (see e.g. Saunders et al. 1992 for IRAS galaxies that have $r_0 \sim 3.8\ h^{-1}$ Mpc). At higher ($z \sim 1$) redshift even lower correlation lengths have been observed for star forming galaxies: Adelberger et al. (2000) find that *balmer break* ($z \sim 1$ star forming) galaxies have $r_0 \lesssim 3\ h^{-1}$ Mpc, while the blue starburst selected field galaxies at $0.8 < z < 1.5$ have $1 \lesssim r_0 \lesssim 2.5\ h^{-1}$ Mpc (Carlberg et al. 1997; Hogg et al. 2000).

In Fig. 1 we calculate the width of simple top-hat redshift distribution that can reproduce the ERO observed angular amplitude, as a function of r_0. Requiring that EROs have a correlation length of $r_0 \lesssim 3\ h^{-1}$ Mpc, typically measured for $z \sim 1$ star forming galaxies, would imply a very narrow ERO redshift distribution of width $\Delta z \approx 0.05$ to reproduce the observed amplitude, which seems implausible. For any reasonably broad redshift distribution a much larger r_0 is inferred, favoring the larger r_0 known for local early-type galaxies, but irreconcilable with the small correlation lengths observed for star forming galaxies at both low and high-z.

In the remainder of the paper the selection functions expected for distant early type galaxies will thus be used.
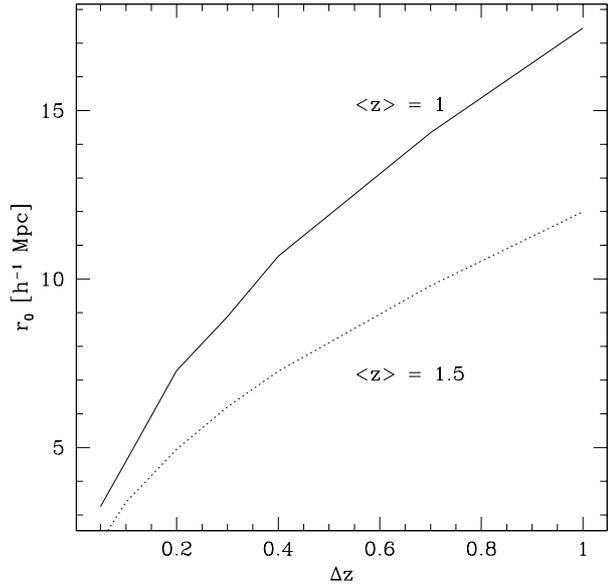
Fig. 1. The correlation length r_0 that reproduces the typical ERO clustering of $A = 0.02$ (D2000), as a function of the width of a top-hat redshift distribution centered at $z = 1$ (solid line) and $z = 1.5$ (dotted line), for the Λ-flat cosmology.

3.1. Modeling the selection function

We adopt models accounting only for passive evolution, appropriate for early-type galaxies, to estimate the ERO selection function. This is well justified for the present analysis that deals with the clustering of galaxies redder than $R - Ks > 5$, corresponding to $z \gtrsim 0.8$–0.9 for a passively evolving L^* elliptical, as several studies have shown that at least up to $z \sim 1$ the photometric and density evolution of the elliptical galaxies is consistent with passive evolution with no number density evolution (Totani & Yoshii 1997; Franceschini et al. 1998; Schade et al. 1999; Im et al. 1999; Broadhurst & Bouwens 2000; Scodeggio & Silva 2000; Phillipps et al. 2000; Daddi et al. 2000a).

For the passive evolution models adopted here, ellipticals form with a rapid burst ($\tau_{\mathrm{SFR}} = 0.1$ Gyr). The Salpeter IMF is assumed, with no dust reddening, and $Z = Z_\odot$. The Bruzual & Charlot spectral synthesis models (1993) in the 1997 version were used, with the Marzke et al. (1994) pure-ellipticals luminosity function for the normalization at $z = 0$. Daddi et al. (2000a) showed that such models reproduce very well the ERO number counts in the range $18 \lesssim K \lesssim 20$, consistently with no appreciable evolution in number density up to $z \sim 1.3$. In Fig. 2 we show some examples of the redshift selection functions of $R - Ks > 5$ ellipticals, as derived from our models, with various formation redshift and limiting Ks magnitude.

In conclusion, we have modeled the selection function accounting only for passive evolution, since empirically the currently available best data including our own sample, indicate little (if any) density evolution and SED's and color trends consistent with pure passive evolution. Some uncertainty exists at $z > 1.5$ where negative density evolution could reduce the numbers of red objects in a magnitude
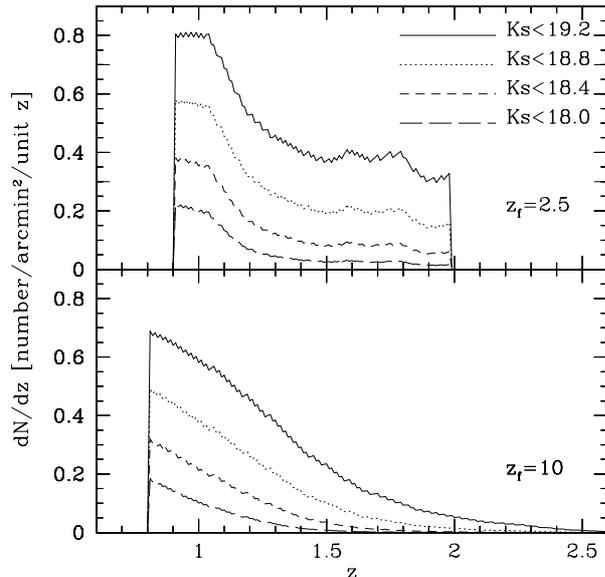
Fig. 2. The selection functions of the ellipticals with $R-Ks > 5$ for the passively evolving model described in the text are shown, for $z_f = 2.5$ (top) and $z_f = 10$ (bottom), and for various Ks limiting magnitudes, for the Λ-flat cosmology.

limited sample, if merging has been important. However, the selection functions we obtain by setting z_f from 2.5 to 30 bracket a large range of possible models and the difference between these in terms of the high-z tail shown in Fig. 2 and used in recovering r_0, may be reasonably expected to accommodate any modest density evolution like that claimed in the models of Kauffmann et al. (1999), Somerville et al. (2001). In fact, there are two features of the selection function that mostly influence the estimate of r_0, i.e. the width Δz and the effective redshift $z_{\rm eff}$ (see Fig. 2). Actually, the two limiting cases of $z_f = 2.5$ or $z_f = 10$ shown in Fig. 2, produce only a modest $\sim 10\%$ variation in the r_0 estimate, basically because the two effects conspire to cancel each other (see Table 1).

4. Estimating the spatial correlation length with Limber's equation

In D2000, clustering amplitudes for EROs with $R-Ks > 5$ were estimated at several Ks limiting magnitudes (Fig. 3, see also Table 5 of D2000). By using the passive evolution dN/dz distribution appropriate for the different Ks limit, the predictions for the angular clustering amplitude have been derived at the same Ks limits by means of Eq. (4), as a function of the r_0 values. The best estimate for r_0 was than obtained from a χ^2 minimization between all the predicted and observed angular clustering amplitude (Fig. 3).

Table 1 reports the inferred results, for different cosmological models and redshift of formation. The table shows that for any given cosmology the best fit values for r_0 are not a strong function of the unknown formation redshift. For each cosmology the worst agreement, as judged from the χ^2 values (see also Fig. 3) is obtained with the
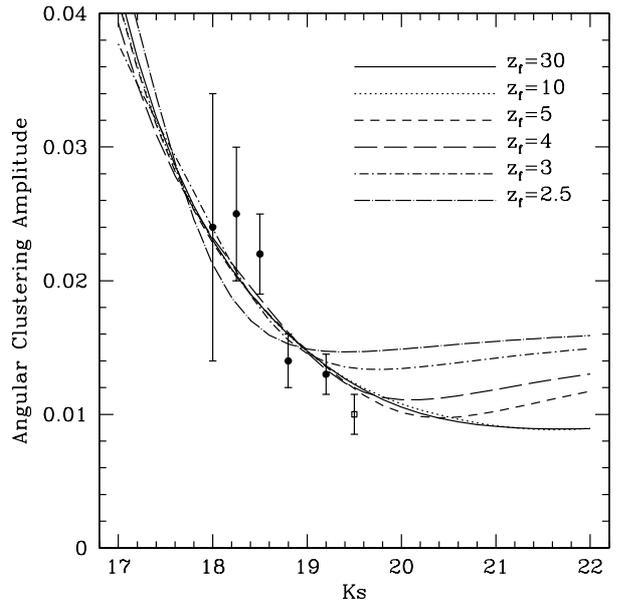
Fig. 3. The data are the angular clustering measurements taken from D2000 (Table 5, filled circles). The empty square is the McCarthy et al. (2000) measurement with H converted to Ks using $H - Ks = 1$. The passive evolution models predictions are also shown, in the case of a Λ-flat cosmology. The r_0 value adopted for each model is the best fitting one, as shown in Table 1. The general trend shown here is unchanged in different cosmologies.

Table 1. Real space correlation lengths for EROs, derived through Limber's equation, assuming the selection functions expected for the ellipticals in the passive evolution case. The correlation lengths r_0 are expressed in comoving h^{-1} Mpc, but a proper scaling to h values different from those used in the models would require a recalculation of the selection functions.

	Λ-flat		open		Ω-flat	
z_f	r_0	$\chi^2_{\min}$	r_0	$\chi^2_{\min}$	r_0	$\chi^2_{\min}$
2.5	14.1	7.1	10.6	10.5	8.3	12.0
3	14.6	3.6	12.5	4.2	10.3	10.3
4	14.3	3.1	12.3	1.9	11.7	6.5
5	13.9	3.7	11.6	2.3	12.3	3.8
10	13.3	3.7	11.3	3.7	11.8	2.2
30	12.9	3.6	11.4	3.4	11.2	3.0

smallest value of z_f. For each entry in the table we estimate a typical error of the order of $\Delta r_0 \lesssim 1\ h^{-1}$ Mpc, obtained by propagating the measured ΔA values through Eq. (4), for the three single most precise A measurements (the error corresponding to a $\Delta\chi^2 = 1$ variation are significantly smaller than that). Given the small variations of r_0 in Table 1, as deduced with different formation redshifts, and their internal variance, we can conclude that, according to the Limber equation, EROs have a comoving correlation length of $r_0 \sim 13.8 \pm 1.5\ h^{-1}$ Mpc in the Λ-flat case, or $r_0 \sim 11.5 \pm 1$ in the open or Ω-flat case, applying to an effective redshift of $1 \lesssim z_{\rm eff} \lesssim 1.2$.

Figure 3 shows that the dependence of A on the Ks limiting magnitude is consistently reproduced by the dN/dz variations, so that the effective correlation length
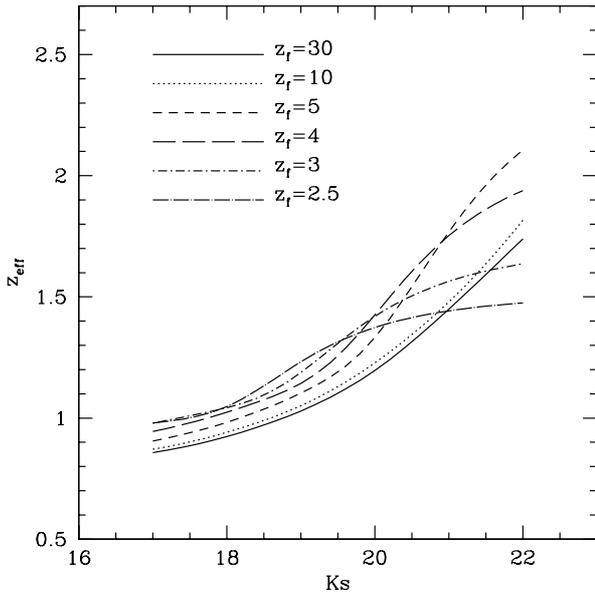
Fig. 4. The variation of the effective redshift $z_{\rm eff}$ (defined in Eq. (6)) for samples of passively evolving ellipticals, selected with $R - Ks > 5$, as a function of the Ks limiting magnitude, for the Λ-flat cosmology.

is not very dependent on the Ks magnitude within the observed range. This reflects the expected small variation of $z_{\rm eff}$ over our samples (from $z_{\rm eff} \sim 1$ at $Ks = 18$ to $z_{\rm eff} \sim 1.2$ at $Ks = 19.2$, see Fig. 4). We stress that the optimal agreement between the predicted and observed trend of the ERO angular clustering versus limiting Ks magnitude is good evidence of the consistency of our modeling of the selection function based on the passive evolution of the stellar populations.

We also plot in Fig. 3 the angular clustering measurement by McCarthy et al. (2000), converting their limit of $H < 20.5$ by using the typical color of EROs $H - Ks \sim 1$ (Cimatti et al. 1999), and assuming an error on their measurement similar to our best ones, given their total area of 1000 arcmin^2. Their color selection criterion of $I - H > 3$ is roughly consistent with our $R - Ks > 5$. The McCarthy et al. (2000) point is in good agreement, at least within $\approx 1\sigma$, with our model's predictions for $z_{\rm f} > 4$ and with the general trend of amplitude versus limiting magnitude inferred by the D2000 survey.

5. Estimating the spatial correlation length from numerical simulation

Can we trust Limber's equation results, given the known spikey structure of redshift distributions in pencil-beam surveys? The size of our field (22×32 arcmin) corresponds, in fact, to $\sim 17 \times 25 \, h^{-1}$ Mpc at $z = 1$, while in the redshift direction we sample objects over a range of approximately $1000 \, h^{-1}$ Mpc (Λ-flat cosmology). The comoving correlation lengths derived from the Limber equation analysis is therefore of the same order of the projected size of our survey, suggesting that a very clumpy redshift distributions should be expected for our sample. As Limber's equation

has formally no dependence on the extension of the field over which the angular correlations are measured, we expect that it should apply in the limit in which the analyzed field of view is large enough so that the observed redshift distribution approaches the selection function. But it is not clear a priori if the Limber's equation should apply accurately for small fields of view, in which the sampling of redshifts along the line of sight will vary considerably, dominated by notable spikes (e.g. Broadhurst et al. 1990; Cohen et al. 1999; Yoshida et al. 2001).

Since this point has not been investigated previously we have embarked upon detailed modeling with realistic simulations. To do this we created clustered 3D distributions of objects with known input r_0 in a suitable comoving volume, we then applied the selection function dN/dz to these simulated data and projected them on the sky for directly measuring the two-point angular correlation function for comparison with the data.

To build up the 3D clustered samples the Soneira & Peebles (1977, 1978) algorithm was used with a 15 level hierarchy, setting the first pass radius equal to $50 \, h^{-1}$ Mpc and the step distance of the algorithm to the proper value to obtain correlations with $\gamma = 1.8$. We refer to the original papers for details and discussions about the algorithm. By directly measuring the 3D two-point functions we calibrate the algorithm's parameters in order to reproduce the desired r_0 value. Such measurements were done by a simple generalization to 3D, following the approach summarized in D2000. The precision we reach is better than $r_0/\Delta r_0 \gtrsim 50$ over the range $6 \lesssim r_0 \lesssim 15$.

The simulations were aimed at reproducing the observations for the EROs with $Ks \leq 18.8$ for which we estimate an angular correlation of $A = 0.014 \pm 0.002$, as this uses the full 701 arcmin^2 area (the measurement at $Ks = 19.2$ has a better S/N but is limited to a smaller area of 447.5 arcmin^2). Given that the analysis based on Limber's equation show that different $z_{\rm f}$ and different cosmologies yield very similar results, we restricted our simulations to the case of dN/dz produced by the model with $z_{\rm f} = 4$ and adopted a Λ-flat cosmology. The idea is to build up a test case to better understand the behavior of projected clustering since we do not expect this to depend significantly on the details of the selection function.

We have produced 120 independent realizations of a field of view of 22×32 arcmin to match the data, for each of 33 values of r_0 ranging from about $6 \, h^{-1}$ Mpc to $15 \, h^{-1}$ Mpc, and then we have measured the angular clustering in the same way as for the data (basing on the Landy & Szalay 1993 estimator, see D2000). The simulations are populated in such a way to produce on average 280 objects for each field to match the data for the EROs with $Ks \leq 18.8$. In Figs. 5 and 6 we show some examples of simulated sky projections together with their corresponding redshift distributions, for a population with $r_0 = 12 \, h^{-1}$ Mpc (that we show in Sect. 5.3 to be the best fitting value for EROs).

The main results of the simulations are shown if Fig. 7. These simulations show two interesting findings. First, the
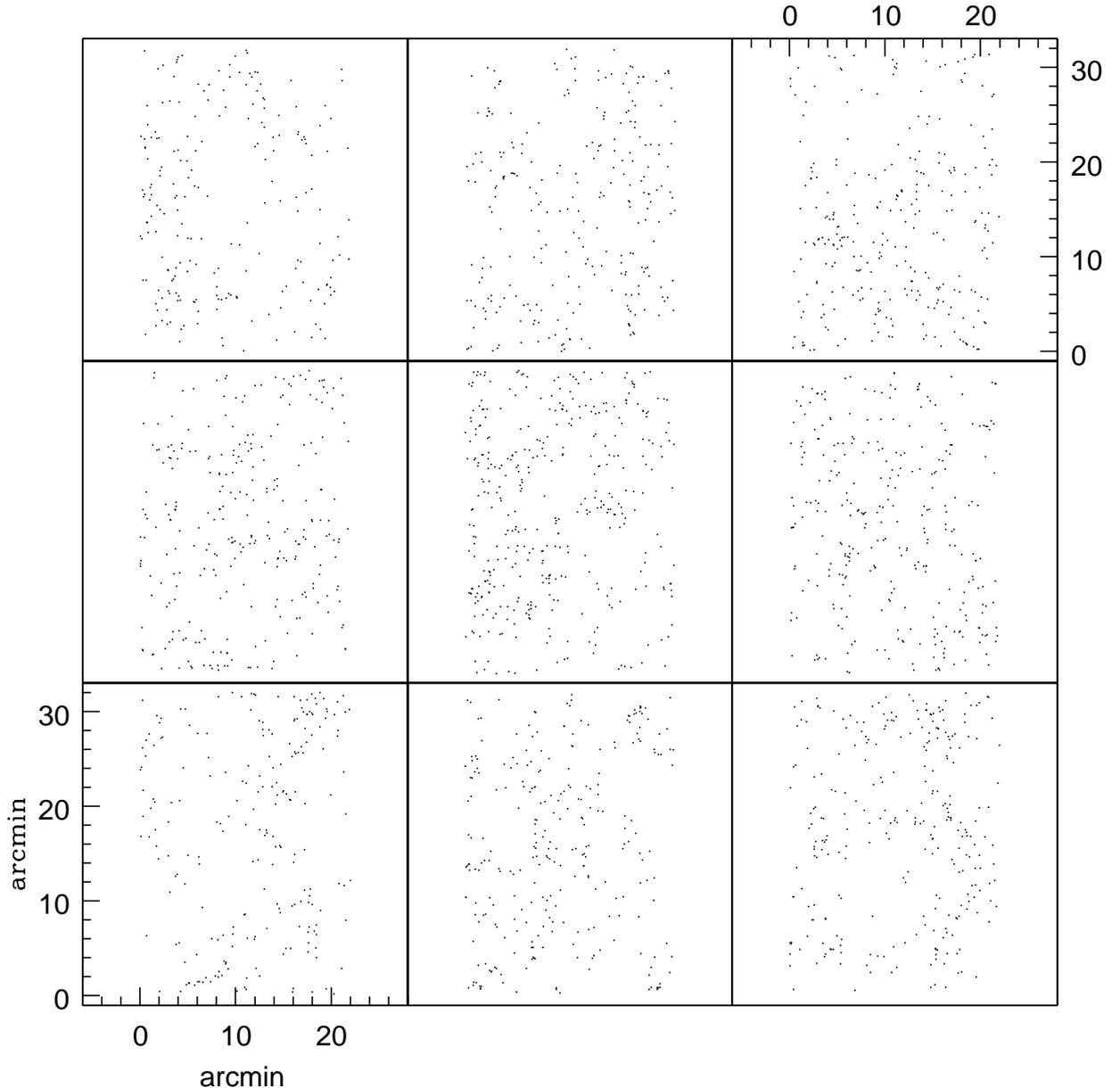
Fig. 5. Examples of simulated realizations of our field of 22×32 arcmin populated with a population with fixed 3D clustering $r_0 = 12 \ h^{-1}$ Mpc. For reference, the top-right panel show the sky distribution of our data.

presence of a large dispersion in the measured values of the amplitude of the correlation function, for any given assumed r_0 value. This in turns implies, for any given measured amplitude, a large range for the statistically acceptable values for r_0, well in excess of what obtained from the Limber's equation (see previous section). Secondly, for each r_0 value the mean clustering amplitude recovered from the simulations is systematically higher than what predicted by the Limber's equation.

5.1. Intrinsic variance of the two-point correlation function

The origin of both these effects (large dispersion and bias of the amplitude of the correlation function) can be estimated from simple considerations. The basic line of

reasoning is the well known fact that, because of clustering, the actual variance in the object number counts is larger than the poissonian variance, and can be written as (see D2000, Eq. (8)):

$$\sigma_n^2 = \overline{n} \left(1 + \overline{n} AC \right) \tag{8}$$

where $\overline{n}$ is the mean expected number of objects and AC is the integral constraint (Groth & Peebles 1977):

$$AC = \frac{1}{\Omega^2} \int \int w(\theta) \mathrm{d}\Omega_1 \mathrm{d}\Omega_2. \tag{9}$$

The expression for the variance in Eq. (8) is the same which one would obtain if all the observed objects would belong to clumps with:

$$N_{\mathrm{cl}} = (AC)^{-1} \tag{10}$$

Fig. 6. Examples of redshift distribution recovered from the simulations. Each panel refers to the corresponding one in Fig. 5. In the top-right panel the adopted selection function is shown.

Fig. 8. The filled squares show the standard deviation versus the mean angular amplitude recovered from the simulations. Empty squares are the average statistical uncertainties in the A measurements. The solid line corresponds to the predictions of Eq. (12), while dashed line is obtained by adding in quadrature both sources of variance.

variance in the clustering amplitude A. In the minimal hypothesis that the clumps are distributed at random in the sky (i.e. neglecting the clustering between clumps) then:

$$\sigma_{N_{\rm cl}} \equiv \sqrt{N_{\rm cl}} \equiv \frac{\partial N_{\rm cl}}{\partial A} \sigma_A \qquad (11)$$

from which it follows that the relative dispersion on the amplitude of the correlation function caused by the sky fluctuation of $N_{\rm cl}$ would be:

$$\frac{\sigma_A}{A} = \sqrt{AC}. \qquad (12)$$

Thus, one should observe a real variation of the correlation amplitude A on the sky, even at fixed 3D clustering length. The observations of angular clustering for a population of fixed r_0 should result in a distribution of values with a variance decreasing with the area over which the measurements are carried out (the factor C is a decreasing function of the area, see Eq. (9) in D2000), and strongly increasing with the expected average angular amplitude ($\sigma_A \propto A^{3/2}$).

In any generic angular clustering measurement such *intrinsic* variance, that depends on the survey geometry and the clustering strength, has to be added to the statistical uncertainty in the measurement of A that is linked to the finite number of observed galaxies. In principle with very large areas (and/or weak clustering) only the latter has a measurable effect, but in the case of small fields, if the clustering itself is strong, the former may become the dominant source of uncertainty.

Our analytical derivation is supported by and can explain the results of the simulations that we have carried

Fig. 7. The data points show the mean angular clustering amplitude recovered from the simulations, as a function of the input r_0. The error bars correspond to the standard deviation of the distribution of the recovered amplitudes. For comparison, the predictions of the Limber's equation are shown (curved line). The shadowed area brackets our observed amplitude and its uncertainty $A = 0.014 \pm 0.002$.

(i.e., from Eq. (9), the number of clumps is the inverse of the average of $w(\theta)$ over the observed field), and the number of objects per clump were a stochastic variable with average $\overline{n}/N_{\rm cl}$. From Eq. (10) it is expected that a variance in the number of clumps $N_{\rm cl}$ should result in a

Fig. 9. The same of Fig. 7, but for a field of 7000 arcmin^2.

Fig. 10. The probability to produce an ERO angular amplitude $A > 0.014$ as a function of the correlation length r_0. The dashed lines show the 1σ range for r_0.

out. Figure 8 shows that only by adding both contributions, the variance measured in the simulations can be recovered rather well, with some underestimation ($\lesssim 10\%$) for large A values. Probably such small underestimation is explained by other effects neglected here, such as for instance the variance in the mean redshift of the clumps in a given beam, as the angular clustering is increased for a lower mean redshift. Incidentally, we note from Fig. 8 that the statistical uncertainty in each single measurement of A is found to be rather constant as a function of A, thus depending only on the number of observed objects. At the same time such statistical uncertainty seems to be overestimated by a factor of ~ 2 (we recall that it follows from assuming 2 sigma Poisson errors for the correlations as suggested by bootstrap analyses, see the discussion about it in D2000), given that $\lim_{A\to 0} \sigma_A$ is about half of the average statistical uncertainty in the measurements of A (see Fig. 8).

The basic results of this analysis is that the variance in the angular clustering can be much larger than the purely statistical variance, especially for small fields of view. A similar qualitative conclusion was empirically reached by Postman et al. (1998) by splitting their large photometric survey into 250 smaller subunits, finding a large scatter in the amplitudes recovered from the smaller fields; a point taken up by McCracken et al. (2000) in the analysis of a single very deep field of 50 arcmin^2. For the first time here we quantify this effect and give a general analytical prescription to predict its amplitude. In the literature this additional source of variance is usually not considered, while deprojection analyses have been carried out even for surveys covering tiny fields of view of only a few arcmin^2 of sky (e.g. from the Hubble Deep Fields) which must severely underestimate the true variance if the standard Limber's based inversion procedure is applied. Moreover, as a large variance is indeed expected for the
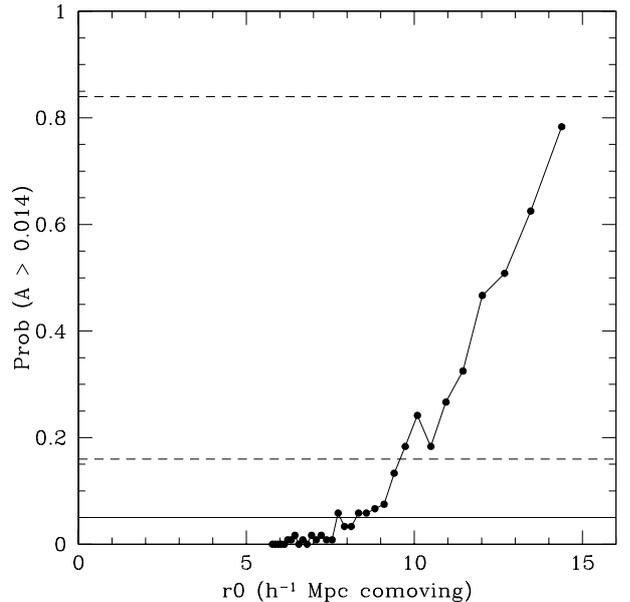
measurements of A, our findings may help to explain why so many apparently discrepant clustering measurements (for similar observing conditions) have been found in the literature (see e.g. Fynbo et al. 2000; McCracken et al. 2000).

5.2. A possible bias in the Limber's equation based inversion

The other interesting finding of our simulations is the possible presence of a small (about 15%) but significant bias, with respect to Limber's equation predictions on the relation between r_0 and the measured angular correlation amplitude (Fig. 7).

Also this effect can be understood by thinking in terms of objects coming in clumps, with A and $N_{\rm cl}$ linked by Eq. (10). In fact, since in general $< \frac{1}{N_{\rm cl}} > \; \neq \frac{1}{<N_{\rm cl}>}$, because of Eq. (10) we should expect deviations of $< A >$ from the Limber's equation predictions if $N_{\rm cl}$ is small or if the distributions of $N_{\rm cl}$ is significantly skewed. The inverse of A (proportional to $N_{\rm cl}$) should instead be less affected, and in fact we find that the average of the *inverse* of A is in better agreement with Limber's equation predictions. This effect is anyway small compared to the huge variance and so for our sample it is not an important correction. We have examined the possibility that this bias is at least in part produced by our calculation procedures generating some systematic effect, such for instance a bias in our estimator (Hewett 1982; Kerscher et al. 2000) or an overcorrection for the integral constraint. To rule out this possibility we built up uncorrelated (random) samples with the same average number of objects and measured their two point angular correlations. This results in an amplitude of $A = 1.4 \times 10^{-4} \pm 1.2 \times 10^{-3}$, thus showing that

possible systematic effects on the estimation of A are much smaller than the bias we find. To verify further this point we carried out simulations as in Sect. 5, over a larger area of 7000 arcmin^2 area (i.e. 2 square degrees, 10 times larger than our ERO field) keeping the surface density of objects fixed at the observed level. This exercise confirms the presence of some bias although, as expected, at a lower level, and still increasing with increasing r_0 suggesting that it is a real effect (Fig. 9). This larger simulation also allowed us to verify that the trend predicted by Eq. (12) still holds correctly.

5.3. Application of the simulations to EROs

From Fig. 7 it can be seen that the ERO observed clustering amplitude $A = 0.014 \pm 0.002$ corresponds to $r_0 \sim 12 \pm 3 \ h^{-1}$ Mpc. This is considerably different from the simple Limber's equation estimate of $r_0 \sim 13.2 \pm 0.8$ which we infer underestimates the uncertainty in the clustering amplitude by a factor of ~ 3. Thus, the cosmic variance is a substantial source of uncertainty in the r_0 estimate for EROs, reducing the weight of the possible uncertainties in our selection function modeling. Using the spread in the A measurements from the simulations shown in Fig. 7 we may place a lower limit to the correlation length of $r_0 \gtrsim 8 \ h^{-1}$ Mpc (see Fig. 10) at the 95% confidence level. While this estimate is derived only from the measurement at $Ks = 18.8$, we expect it to be consistent with what we would have found from the analysis of the clustering at all Ks levels. This is because within each single survey the number (and the redshift) of the clumps is fixed in the real space, so that we expect that the trend of the clustering amplitude as a function of the apparent magnitude should basically reflect only the change of the redshift distribution (see Fig. 3).

Our simulations have been carried out for convenience for the Λ–flat universe. From the results of Sect. 4 we can say that in the open or Ω–flat cases the r_0 estimate is lower by a small amount, so that at the 95% confidence level it becomes $r_0 \gtrsim 7 \ h^{-1}$ Mpc.

Figure 3 shows that the angular clustering measurement of McCarthy et al. (2000) is consistent with our measurements, even if slightly lower than our model predictions. Given the large variance expected, the discrepancy is not significant. Nevertheless McCarthy et al. (2000) estimate from their data $r_0 \sim 8 \ h^{-1}$ comoving Mpc, significantly lower than our preferred r_0 value. The main reason for this lower r_0 value is in their adoption of a relatively narrow Gaussian form of dN/dz, centered at $z = 1.2$ and with $\sigma_z = 0.15$, motivated by their photometric redshift estimates. Such a strong confinement of EROs into a narrow redshift range is not in agreement with our modeling of the selection function shown in Fig. 2. Even if Fig. 6 demonstrates that occasionally in small fields the observed dN/dz could be spuriously narrow (because of the clustering), the inversion process requires the use of the actual selection function, which we expect to be much broader than

the observed, clumpy dN/dz of a given field. Assuming that the McCarthy et al. threshold of $I - H > 3$ is consistent with $R - Ks > 5$, and using our estimate of the ERO selection function at $Ks < 19.5$, the McCarthy et al. angular measurement could be inverted to $r_0 = 10.8 \pm 2.2$, where the uncertainty is derived from our own one by keeping into account the scaling with the area and clustering amplitude, consistently with Eq. (12). This estimate apply to an effective redshift $z_{\text{eff}} \sim 1.2$ (Fig. 4).

6. Discussion

6.1. Comparison to the clustering of bright local ellipticals

We now compare the large correlation length estimated for the $z \gtrsim 1$ ellipticals with that of their local counterparts, in order to constrain the cosmic evolution of the clustering of massive early-type galaxies.

The correlation length of a population of galaxies is known to depend on the absolute luminosity selection threshold, and can also depend on the scales over which the clustering is measured. Such quantities must be properly estimated in order to compare the clustering of EROs to that of local ellipticals. For a passively evolving elliptical, the apparent magnitude of $Ks = 19.2$ corresponds to $L \sim 0.6L^*$ and $L \sim 1.3L^*$ at the redshift of 1 and 1.5, respectively, while for $Ks = 18$ we have $L \sim 1.6L^*$ at $z = 1$ and $L \sim 4L^*$ at $z = 1.5$ (accounting for the passive evolution of L^*). Therefore our sample consists of galaxies with typical luminosity $L \gtrsim L^*$. The largest effective separation probed by our angular clustering measurements is $\theta \simeq 15'$, corresponding to about $12 \ h^{-1}$ Mpc at $z \sim 1$ (Λ–flat universe).

As the clustering amplitude is expressed with r_0^γ, the measurements of r_0 obtained with a γ different from the value adopted here must be rescaled to that value in order to produce a meaningful comparison. Therefore, all the r_0 quoted below were transformed with $\gamma = 1.8$.

Our results can be compared with those obtained locally, for two different samples, by Guzzo et al. (1997, the Perseus Pisces redshift survey) and Willmer et al. (1998, the SSRS2 redshift survey). Both estimate the clustering of bright early type galaxies with $M_B < -19.5 + 5 \log h$, corresponding to $L \gtrsim L^*$. Guzzo et al. measure scales up to about $10 \ h^{-1}$ Mpc and find $r_0 = 11.3 \pm 1.3 \ h^{-1}$ Mpc, while Willmer et al. measure up to about $20 \ h^{-1}$ Mpc and find $r_0 = 7.6 \pm 1.2$. The two measurements are only consistent with each other at the 2σ level, but it should be noted that the Perseus Pisces redshift survey has a higher abundance of local clusters. It may be implied by Fig. 10 of Willmer et al. (1998) that they would obtain a larger amplitude if limited to smaller separations. For further constraints we note that local radio galaxies, known to be hosted by bright ellipticals, have $r_0 = 11 \pm 1.2 \ h^{-1}$ Mpc (Peacock & Nicholson 1991). Therefore a correlation length in the range $r_0 \sim 9$–$11 \ h^{-1}$ Mpc can

be regarded as a reasonable estimate for the clustering amplitude of local $L \gtrsim L^*$ ellipticals.

Our estimate of $r_0 = 12 \pm 3 \; h^{-1}$ Mpc then implies that the clustering amplitude of bright ellipticals does not significantly increase from to $z \sim 1 - 1.5$ to the present. The *stable clustering* scenario (i.e. $\epsilon = 0$, if $r_0(z) = r_0(z = 0)(1 + z)^{(\gamma-3-\epsilon)/\gamma}$) that is known to fit many observations of clustering evolution to $z \sim 1$ (e.g. Peebles 1980; Le Fevre et al. 1996; Carlberg et al. 1997), would predict $r_0 \sim 6 \; h^{-1}$ Mpc at our inferred effective redshift of $z_{\mathrm{eff}} \sim 1.1$ and hence it is not in good agreement with our measurement of the ERO clustering. A negative value for ϵ is supported by our analysis.

6.2. Comparison to theoretical predictions

The evolution of the correlation function is popularly characterized as:

$$\xi(z, r) = D^2(z)b^2(z)\xi_{\mathrm{mass}}(0, r) \qquad (13)$$

where the purely linear growth $D(z)$ of density perturbations, $\Delta\rho(z)/\rho(z)$, is separated from the bias evolution $b(z)$. In the linear case the bias evolution can be expressed with the Tegmark & Peebles (1998) prescriptions and well known expressions for the linear growth factor can be assumed (Peebles 1980; Treyer & Lahav 1996). In our case the linear assumptions are not likely to be correct, as for EROs we are mapping angular comoving scales similar to the inferred r_0, thus sampling a region with $\xi \sim 1$, so that this prescription can be considered as a rough benchmark picture in the absence of the complexities affecting small scale growth (Kauffmann et al. 1999; Somerville et al. 2001).

The simplest and most clear model of bias evolution of ellipticals is provided by the so called *galaxy conservation* scenario (Fry et al. 1996; Tegmark & Peebles 1998; Moscardini et al. 1998; Magliocchetti et al. 1999; Lacy 2000), that holds if the galaxy population is conserved over the cosmic time (i.e. no new elliptical forms and no one disappears). This scenario implies the assumption that all the ellipticals were formed at high redshift and simply follow the growth of perturbations without the additional non-linear effects such as virial collapse and merging expected at small scales (below r_0 of the mass auto-correlation function). It is therefore relevant as a limiting case for comparison with our observations. Here the positive evolution of the bias which increases with redshift is more than compensated by the decline of linear growth, i.e. $D(z)$ wins and a net decline of the clustering amplitude with increasing redshift is expected in the linear regime beyond r_0 of the mass-autocorrelation function.

In Fig. 11 (Λ-flat case) we see that normalizing the linear predictions to the r_0 and bias of local ellipticals (such bias was computed assuming $r_0 = 10 \; h^{-1}$ Mpc and the normalization $\sigma_8^{\mathrm{mass}} = 0.9$, from Eke et al. 1996), the predicted trend is slightly decreasing in comoving units, reaching values around $r_0 \sim 7$–$8 \; h^{-1}$ Mpc at $z = 1.1$.
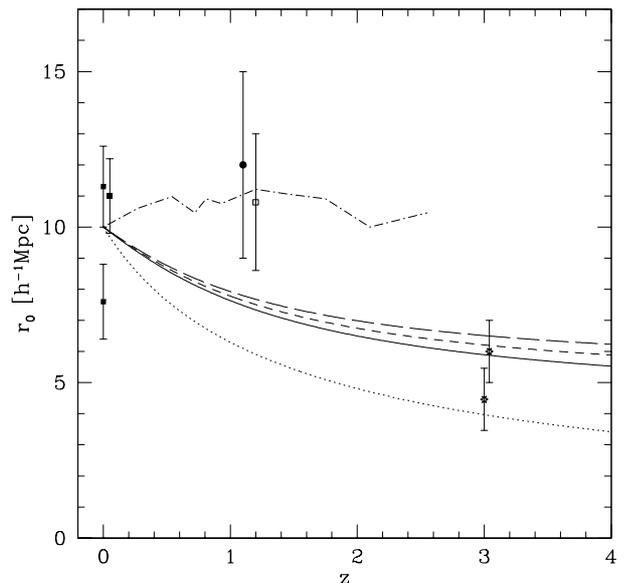
Fig. 11. The r_0 measurements for local ellipticals (filled squares), $z \sim 1$ ellipticals (EROs; filled circle from D2000; the empty square is derived from our analysis applied to the McCarthy et al. angular clustering measurement) and LBGs (asterisks) are shown for the Λ-flat universe (see the text for details). The dot-dashed line shows the Kauffmann et al. (1999) ΛCDM predictions for the clustering of ellipticals. The case of stable clustering ($\epsilon = 0$) is indicated by the dotted line. The other three curves show the predictions for the *galaxy conservation* scenario, differing in the assumed degree of correlation between galaxy and dark matter, assumed from top to bottom to be 0.9–0.95–1 at $z = 0$ (see Tegmark & Peebles 1998, for more details on this parameter). All the models were normalized to $r_0(0) = 10 \; h^{-1}$ Mpc.

Given the large uncertainties, this scenario cannot be rejected with great confidence, but it is disfavored by our findings.

If the *galaxy conservation* model predictions, both for the bias and for r_0, are extended to higher z, they do intercept the measurements for the LBGs clustering by Giavalisco et al. (1998) and Adelberger et al. (1998) (see Fig. 11 for the Λ-flat case). This kind of argument had led to previous suggestions that LBG's could evolve into present-day bright ellipticals (e.g. Adelberger 2000). An important confirmation of this picture would be to find that distant (i.e. $z \sim 1$) ellipticals have intermediate clustering strength between the local ones and the LBGs. Our findings, taken at face value, disfavor such an interpretation as they seem to suggest that the clustering of ellipticals is not decreasing enough from $z \sim 0$ to $z \sim 1$ to reproduce the clustering at $z = 3$, at least for the LBGs with absolute luminosity similar to those in the Giavalisco et al. (1998) and Adelberger et al. (1998) samples.

Alternative more complex models for the clustering evolution have been constructed to deal with nonlinear effects and may be termed the *galaxy merging* scenario for bias evolution (e.g. Mo & White 1996; Moscardini et al. 1998), in which the bias grows with z with some law of the

kind $\Delta b \propto (1+z)^{1.8}$, which is stronger than the growth of perturbations, with the net effect that r_0 increase with z. Such models are in better agreement with the ERO clustering, especially if the large favored $r_0 \sim 12$ h^{-1} Mpc will be confirmed. Similar predictions for the clustering evolution of the ellipticals in the ΛCDM semianalytic model of Kauffmann et al. (1999) and Somerville et al. (2001) are also consistent with the trend inferred here (see Fig. 11) and include further refinements such as luminosity evolution.

A difficulty one might expect of strong bias evolution models is that they may contradict the observational evidence of the lack of evolution of the comoving density of ellipticals, which appears not to decrease significantly to $z = 1$ and beyond (see Daddi et al. 2000a). However, depending on the details of the semi-analytical approach, it is possible to accommodate substantial bias evolution of the dark matter without perturbing either the apparent space density or clustering amplitude of elliptical galaxies for the ΛCDM model (Kauffmann et al. 1999; Somerville et al. 2001, see also Bullock et al. 2001) and the main difference between these models and the conservation scenario would seem to be the inclusion of a suitable prescription for merging. As discussed in Daddi et al. (2000a), the small amount of density evolution required by the ΛCDM models could be consistent with the ERO number counts once it is required that merging does not produce significant star formation (that would make the objects bluer than our color cuts), i.e. *red merging* is required. This indeed is claimed to have been observed in clusters (van Dokkum et al. 2001).

7. Summary and conclusions

The main results presented in this paper are:
• The real space correlation length of EROs (with $R - Ks > 5$) is much larger that the correlation of $z \sim 1$ star-forming galaxies for any reasonably large selection function, strengthening the previous suggestions that most EROs at $Ks \sim 19$ are early-type galaxies.
• Assuming that EROs are predominantly early-type galaxies and hence that their selection function is reasonably described by passive evolution, then the spatial correlation length we obtain is rather large, not less than 7–8 h^{-1} Mpc, with the most probable estimate of 12 ± 3 h^{-1} Mpc, applying to an effective redshift of $z \sim 1.2$.
• At face value this implies no significant evolution of clustering of this population relative to the present day when measured in *comoving coordinates*, and a strong bias increase from $z = 0$ to 1.
• Realistic simulations were used to constrain r_0 from the observed angular clustering of EROs. Two main results follow from the simulations that can be of general interest for the analysis of the angular clustering: (1) the amplitude A of the angular two-point correlation function fluctuates on the sky according to $\sigma_A/A = \sqrt{AC}$, and (2) a possible systematic overestimate of r_0 could

follow from the inversion of the angular clustering measurements based on Limber equation. Both effects are strongly enhanced in the limits of strong angular clustering and/or small fields of view.

Taken at face value, our result on the ERO correlation length challenges the simple conservation models of clustering growth for massive haloes, but it may be reconciled with more complex schemes for the bias which incorporate more parameters to describe non-linear effects such as merging, so that although evolution of the underlying mass function strongly declines with redshift, the observer will, it is claimed, find the opposite of the expected behavior, namely an increase in the observed correlation length of early-type galaxies with redshift and no corresponding strong decline in their number density with increasing redshift (Kauffmann et al. 1999; Somerville et al. 2001). We rule out a high degree of density evolution of early type galaxies to $z \sim 1$. This is inconsistent with the ERO clustering because strong density evolution would significantly narrow the width of the selection function by removing the high-z tail resulting in a reduction of the inferred estimate of r_0. This is counter to the strongly increasing correlation amplitude that would be expected with increasing redshift for such a highly biased model. A modest reduction in density at $z > 1$ can be accommodated given the present uncertainties in lookback time and star formation which fold into the construction of the selection function. Indeed some change in density through merging is suggested by our results when we combine the constraints on both density and correlation length evolution.

Before discarding the *galaxy conservation* scenario for the clustering evolution of early type galaxies some possible concerns should anyway be carefully considered, that could make the measurement of clustering spuriously high. Firstly if somehow the volume sampled by EROs is over-abundant in rich clusters with respect to the local samples, this would increase r_0. In D2000 we discuss this point, suggesting that it is unlikely and our simulations here support this. Secondly if the EROs are somehow confined to a narrower redshift range than expected on the basis of passive evolution, then the estimate of r_0 should be lowered (McCarthy et al. 2000). This would also have the effect of increasing the comoving density, meaning in turn positive density evolution which would be hard to imagine. Finally, we have evaluated the cosmic variance with our modeling of the true *external* error bars showing that we cannot rule out that both our result and that claimed by McCarthy et al. (2000) are consistent with the *galaxy conservation* scenario, representing a $\approx 1.5\sigma$ high deviation from a true lower correlation length. On the other hand, anyway, if a significant fraction of dusty objects is present among EROs this would probably imply that the correlation length of the genuine early-type fraction could be larger than our estimate.

Much larger areas have to be observed to reduce the error on r_0. Our simulations have shown that the variance of A from spikes is a slowly decreasing function of the area, while the statistical uncertainty in each single A

measurement seems to decrease faster, with the square root of the number of the objects, suggesting that the best strategy to get rid of the Eq. (12) variance (and to increase thus the precision on the estimate of r_0) is to observe many independent and relatively large fields. At the same time the redshifts of complete samples of EROs should be obtained to constrain their selection function. From Fig. 6 we estimate that to observationally establish a detailed ERO selection function will reasonably require thousands ERO redshifts to overcome the problems linked to the existence of clumps.

References

Adelberger, K., Steidel, C., Giavalisco, M., et al. 1998, ApJ, 505, 18

Adelberger, K. 2000, Clustering at High Redshift, ed. A. Mazure, O. Le Fevre, & V. Le Brun, ASP Conf. Ser. 200 [astro-ph/9912153]

Andreani, P., Cimatti, A., Loinard, L., & Röttgering, H. 2000, A&A, 354, L1

Baugh, C. M., Cole, S., & Frenk, C. S. 1996, MNRAS, 283, 1361

Broadhurst, T., Ellis, R., Koo, D., & Szalay, A. 1990, Nature, 343, 726

Broadhurst, T., & Bouwens, R. 2000, ApJ, 530, 53

Bruzual, G., & Charlot, S. 1993, ApJ, 405, 538

Bullock, J., Dekel, A., Kolatt, T., et al. 2001, ApJ, in press [astro-ph/0005325]

Carlberg, R., Cowie, L., Songaila, A., & Hu, E. 1997, ApJ, 484, 538

Cimatti, A. 2001, to appear in the proceedings of the Deep Fields Workshop, Garching [astro-ph/0012057]

Cimatti, A., Andreani, P., Röttgering, H., & Tilanus, R. 1998, Nature, 392, 895

Cimatti, A., Daddi, E., di Serego Alighieri, S., et al. 1999, A&A, 352, L45

Cohen, J., Hogg, D., Blandford, R., et al. 1999, ApJ, 512, 30

Cohen, J., Hogg, D., Blandford, R., et al. 2000, ApJ, 538, 29

Daddi, E., Cimatti, A., & Renzini, A. 2000a, A&A, 362, L45

Daddi, E., Cimatti, A., Pozzetti, L., et al. 2000b, A&A, 361, 535 (D2000)

Davis, M., & Geller, M. 1976, ApJ, 208, 13

Dey, A., Graham, J. R., Ivison, R. J., et al. 1999, ApJ, 519, 610

Dressler, A. 1980, ApJ, 236, 351

Efstathiou, A., Bernstein, G., Tyson, A., et al. 1991, ApJ, 380, L47

Eke, V., Cole, S., & Frenk, C. 1996, MNRAS, 282, 263

Eisenhardt, P., Elston, R., Stanford, S. A., et al. 1998, proceedings of the Xth Rencontres de Blois on The Birth of Galaxies, ed. B. Guiderdoni et al. [astro-ph/0002468]

Franceschini, A., Silva, L., Fasano, G., et al. 1998, ApJ, 506, 600

Fynbo, J., Freudling, W., & Möller, P. 2000, A&A, 355, 37

Fry, J. 1996, ApJ, 461, L65

Gear, W., Lilly, S., Stevens, J., et al. 2000, MNRAS, 316, L51

Giavalisco, M., Steidel, C., Adelberger, K., et al. 1998, ApJ, 503, 543

Guzzo, L., Strauss, M., Fisher, K., et al. 1997, ApJ, 489, 37

Giovanelli, R., Haynes, M., & Chincarini, G. 1986, ApJ, 300, 77

Groth, E. J., & Peebles, P. J. E. 1977, ApJ, 217, 38

Hewett, P. 1982, MNRAS, 201, 867

Hogg, D., Cohen, J., & Blandford, R. 2000, ApJ, 545, 32

Kauffmann, G. 1996, MNRAS, 281, 487

Kauffmann, G., Colberg, J. M., Diaferio, A., & White, S. D. M. 1999, MNRAS, 307, 529

Kerscher, M., Szapudi, I., & Szalay, A., ApJ, 535, L13

Im, M., Simard, L., Faber, S., et al. 2000, ApJ, in press [astro-ph/0011092]

Lacy, M. 2000, ApJ, 536, L1

Landy, S. D., & Szalay, A. S. 1993, ApJ, 412, 64

Le Fevre, O., Hudon, L., Lilly, S., et al. 1996, ApJ, 461, 534

Loveday, J., Maddox, S. J., Efstathiou, G., & Peterson, B. A. 1995, ApJ, 442, 457

Liu, M. C., Dey, A., Graham, J. R., et al. 2000, AJ, 119, 2556

Magliocchetti, M., Maddox, S., Lahav, O., & Wall, J. 1999, MNRAS, 306, 943

Marzke, R. O., Geller, M. J., Huchra, J. P., et al., 1994, AJ, 108, 437

McCarthy, P., et al. 2000, AAS, 197, 6502 (see also [astro-ph/0011499])

McCracken, H., Shanks, T., Metcalfe, N., et al. 2000, MNRAS, 318, 913

Mo, H., & White, S. D. M. 1996, MNRAS, 282, 347

Moriondo, G., Cimatti, A., & Daddi, E. 2000, A&A, 364, 26

Moscardini, L., Coles, P., Lucchin, F., & Matarrese, S. 1998, MNRAS, 299, 95

Peacock, J., & Nicholson, D. 1991, MNRAS, 253, 307

Peebles, P. J. E. 1980, The Large-Scale Structure of the Universe (Princeton University Press)

Phillipps, S., Driver, S., Couch, W., et al. 2000, MNRAS, 319, 807

Postman, M., Lauer, T., Szapudi, I., & Oegerle, W. 1998, ApJ, 506, 33

Roche, N., & Eales, S. 1999, MNRAS, 307, 703

Saunders, W., Rowan-Robinson, M., & Lawrence, A. 1992, MNRAS, 258, 134

Schade, D., Lilly, S. J., Crampton, D., et al. 1999, ApJ, 525, 31

Scodeggio, M., & Silva, D. 2000, A&A, 359, 953

Smail, I., Ivison, R. J., Kneib, J. P., et al. 1999, MNRAS, 308, 1061

Soifer, B. T., Matthews, K., Neugebauer, G., et al. 1999, AJ, 118, 2065

Somerville, R., Lemson, G., Sigad, Y., et al. 2001, MNRAS, 320, 289

Soneira, S., & Peebles, P. J. E. 1977, ApJ, 211, 1

Soneira, S., & Peebles, P. J. E. 1978, AJ, 83, 845

Spinrad, H., Dey, A., Stern, D., et al. 1997, ApJ, 484, 581

Stiavelli, M., & Treu, T. 2000, Proc. of the Conf. Galaxy Disks and Disk Galaxies, ASP Conf. Ser., ed. Funes, & Corsini [astro-ph/0010100]

Tegmark, M., & Peebles, P. J. E. 1998, ApJ, 500, L79

Totani, T., & Yoshii, J. 1997, ApJ, 501, L177

Treyer, M., & Lahav, O. 1996, MNRAS, 280, 469

van Dokkum, P., Franx, M., Fabricant, D., et al. 2001, ApJ, 541, 95

Willmer, C., da Costa, L., & Pellegrini, P. 1998, AJ, 115, 869

Yoshida, N., Colberg, J., White, S. D. M., et al. 2001, submitted to MNRAS [astro-ph/0011212]